Electronic Supplementary Information

On-demand acoustic droplet splitting and steering in a disposable microfluidic chip

Jinsoo Park, Jin Ho Jung, Kwangseok Park, Ghulam Destgeer, Husnain Ahmed, Raheel Ahmad and Hyung Jin Sung*
Department of Mechanical Engineering, KAIST, Daejeon 34141, Korea.
E-mail: hjsung@kaist.ac.kr; Fax: +82 42 350 5027; Tel: +82 42 350 3027

PDMS membrane thickness effects

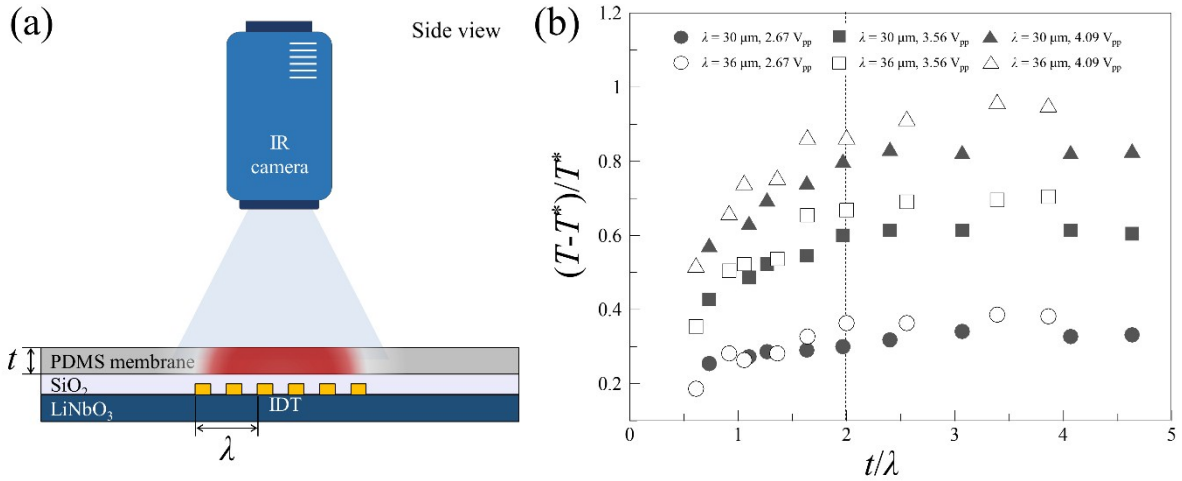

Fig. S1 PDMS thickness effects on acoustic/acoustothermal phenomena; (a) Experimental setup; (b) Results.

The closed PDMS microfluidic chip used in this study comprises a thin PDMS membrane, composed of two posts and a cavity, and a PDMS stamp, where a microchannel is engraved, as in Fig. 1. At the interface between the piezoelectric substrate and the PDMS membrane, surface acoustic waves (SAWs) refract into the membrane in the form of longitudinal waves. As these waves propagate through the viscoelastic medium (PDMS), the acoustic energy attenuates by viscoelastic damping in the cross-linked polymer network. Consequently, the attenuated energy in the form of thermal energy (heat) causes a temperature increase in the PDMS membrane. The amount of the attenuated wave energy is closely related to the membrane thickness and wavelength. Here we measure the temperature increase in the membrane to investigate the wave attenuation phenomenon in the PDMS membrane.

Two kinds of IDTs with different electrode spacing ($\lambda/4$) and thus different resonant frequency ($f_{IDT} = c_s/\lambda$ where c_s is the speed of sound in the $LiNbO_3$ substrate) were used in the experiments. The wavelength (λ; four times the electrode spacing) of the produced acoustic waves was 30 and 36 μm, and the resultant resonant frequency was 120.1 and 99.92 MHz for each IDT, respectively. A thin PDMS membrane with varying thickness (t) was placed on the IDT, which is covered with a SiO_2 layer. The steady-state temperature of the membrane was measured by an IR camera (A325sc, FLIR Systems, USA) at room temperature (T^* = 20ºC), as shown in Fig. S1(a). The $LiNbO_3$ substrate was mounted on a custom-built Peltier cooling system (Photondays Co., Korea) to isolate the heating effect occurring at the substrate and thus to maintain the substrate temperature at room temperature (20ºC). The measurement results in SFig. 1(b) show the normalized temperature increase ($(T-T^*)/T^*$) with respect to the normalized PDMS membrane thickness (t/λ). The black and white symbols indicate the cases of 30 and 36 μm, respectively. The circle, square, and triangle symbols indicate the applied voltage of 2.67, 3.56, and 4.09 V_{pp}, respectively.

As the applied AC voltage (V_{pp}) increased, the temperature increased (from circle to square to triangle symbols). As the membrane thickness increased at a fixed magnitude of the applied AC signals, the temperature linearly increased until $t/\lambda \sim 2$ and remained constant for $t > 2\lambda$. These results imply that the waves were fully attenuated after they travelled along two times the wavelength ($t \sim 2\lambda$). For a PDMS membrane of $t < 2\lambda$ in the closed microfluidic chip, the acoustic field can penetrate through the membrane into the fluid domain. On the contrary, in the case of $t > 2\lambda$, the wave energy is fully attenuated and transformed into thermal energy, leading to acoustothermal heating. These results can also provide plausible explanation for the previously reported closed microfluidic chip-based acoustofluidic devices.[1-3] These SAW-based acoustofluidic devices employed the membrane (alternatively post or pillar) of $t < 2\lambda$ for acoustic manipulation of particles, cells, and droplets. Our previous multichannel droplet sorting device[4] adopted a PDMS membrane of $t \sim 5\lambda$ to utilize the acoustotheraml heating effect to induce thermocapillary droplet migration phenomenon.

Ray acoustics analysis

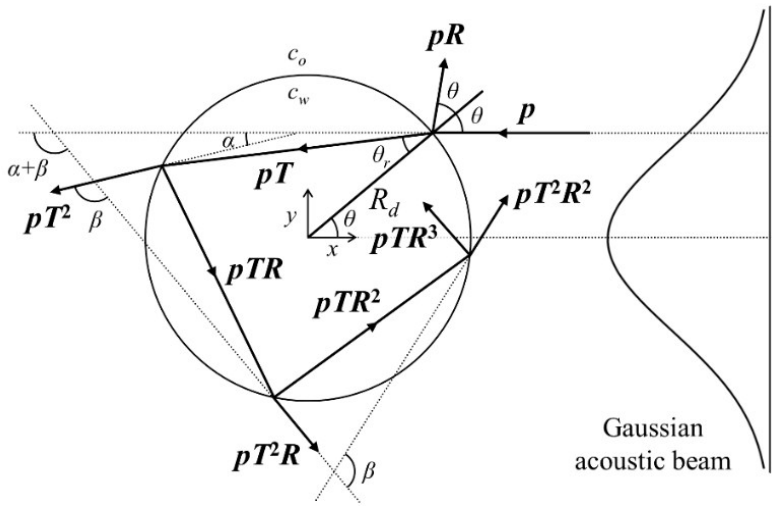

Fig. S2 A single phonon ray path in the ray acoustics analysis

A ray acoustics analysis was conducted for theoretical investigation on the droplet steering phenomenon. The ray acoustics analysis was based on the following assumptions:

1) Ray acoustics regime (Mie scattering where $2R_d > \lambda$), phonon ray momentum (p), incident angle (θ) , refraction angle (θ_r)
The incident angle (θ) was defined with respect to x-coordinate, and the refraction angle (θ_r) was calculated by using the Snell's law such that $c_o sin\theta = c_w sin\theta_r$. For convenient formulation, the angles α and β were defined as $\alpha = 2\theta - 2\theta_r$ and $\beta = \pi - 2\theta_r$, respectively.

2) A coaxial, single acoustic beam with a loosely-focused Gaussian intensity distribution
The longitudinal acoustic wave was assumed to be (i) coaxial to the droplet center, (ii) a single acoustic beam, (iii) loosely-focused where beam waist (w_o) was larger than the wavelength (λ), and (iv) have a Gaussian intensity distribution ($I(\theta)$),

$$I(\theta) = \frac{\sqrt{2}I_o}{\sqrt{\pi w_o^2}} exp\left[\frac{-2R_d^2 sin^2\theta}{w_o^2}\right].$$

3) A cylindrical droplet in Hele-Shaw microchannel ($R_d > h$)
Due to the Hele-Shaw geometry, the droplet interface radius of curvature (R_d) in the xy-plane was significantly larger than that (h/2) in the xz-plane; therefore, the x-propagating component of the waves was only considered while the z-propagating component was neglected for simplicity. The cylindrical water-oil droplet was confined in the microchannel in contact with the four inner walls; thus, the scattering component (F_s) of acoustic radiation force was considered with the gradient component (F_g) neglected.

4) Fresnel reflection (R) and transmission (T) coefficients
The Fresnel reflection and transmission coefficients are defined as:

$$R = \left|\frac{Z_w/cos\theta_r - Z_o/cos\theta}{Z_w/cos\theta_r + Z_o/cos\theta}\right|^2 \text{ and } T = 1 - R,$$ where Z_w and Z_o are acoustic impedance values of the water and oil phases, respectively.

In the ray acoustics analysis, the acoustic wave was regarded as a bundle of acoustic phonon rays carrying momentum (p) as in Fig. S2. The phonon rays (PR, PT^2, PT^2R, PT^2R^2, $\cdots$, PT^2R^n, $\cdots = PR + \sum_{n=0}^{\infty} PT^2R^n$) were scattered at the droplet interface with respective angles ($\pi + 2\theta$, α, $\alpha+\beta$, $\alpha+2\beta$, $\cdots$, $\alpha+n\beta$, $\cdots$). The total acoustic radiation force (F_t), composed of the scattering component (F_s) and the gradient component (F_g) in the x- and y-directions, was attributed to the net momentum change, and they can be formulated as the following:

$$F_s = F_x = \frac{p}{c_o} - \left\{\frac{pR}{c_o}\cos(\pi + 2\theta) + \sum_{n=0}^{\infty}\frac{pT^2R^n}{c_o}cos(\alpha + n\beta)\right\},$$

$$F_g = F_y = 0 - \left\{\frac{pR}{c_o}\sin(\pi + 2\theta) + \sum_{n=0}^{\infty}\frac{pT^2R^n}{c_o}sin(\alpha + n\beta)\right\},$$

$$F_t = F_x + iF_y,$$

$$= \frac{p}{c_o}\{1 + Rcos(2\theta)\} + i\frac{pR}{c_o}\sin(2\theta) - \frac{pT^2}{c_o}\sum_{n=0}^{\infty}R^n\{\cos(\alpha + n\beta) + isin(\alpha + n\beta)\},$$

$$= \frac{p}{c_o}\{1 + Rcos(2\theta)\} + i\frac{pR}{c_o}\sin(2\theta) - \frac{pT^2}{c_o}\sum_{n=0}^{\infty}R^n e^{i(\alpha + n\beta)},$$

$$= \frac{p}{c_o}\{1 + Rcos(2\theta)\} + i\frac{pR}{c_o}\sin(2\theta) - \frac{pT^2}{c_o}\frac{e^{i\alpha}}{1 - Re^{i\beta}},$$

$$= \frac{p}{c_o}\{1 + Rcos(2\theta)\} + i\frac{pR}{c_o}\sin(2\theta) - \frac{pT^2}{c_o}\left[\frac{\cos(2\theta - 2\theta_r) + Rcos(2\theta)}{1 + R^2 + 2Rcos(\theta_r)} + i\frac{\sin(2\theta - 2\theta_r) + Rsin(2\theta)}{1 + R^2 + 2Rcos(\theta_r)}\right],$$

$$F_s = F_x = \frac{p}{c_o}\left[1 + Rcos(2\theta) - \frac{T^2\{\cos(2\theta - 2\theta_r) + Rcos(2\theta)\}}{1 + R^2 + 2Rcos(\theta_r)}\right],$$

$$F_g = F_y = \frac{p}{c_o}\left[Rsin(2\theta) - \frac{T^2\{\sin(2\theta - 2\theta_r) + Rsin(2\theta)\}}{1 + R^2 + 2Rcos(\theta_r)}\right].$$

As a result, the two counteracting forces (acoustic scattering force (F_s) and drag force (F_d)) on the droplet confined in the Hele-Shaw microchannel can be expressed as the following:

$$F_s = \frac{2hR_d}{c_o}\int_0^{\pi/2} I(\theta)\left[1 + Rcos(2\theta) - \frac{T^2\{\cos(2\theta - 2\theta_r) + Rcos(2\theta)\}}{1 + R^2 + 2Rcos(\theta_r)}\right]cos(\theta)d\theta,$$

$$= \frac{2\sqrt{2}hR_dI_o}{\sqrt{\pi}c_ow_o}\int_0^{\pi/2} exp\left[\frac{-2{R_d}^2sin^2\theta}{{w_o}^2}\right]\left[1 + Rcos(2\theta) - \frac{T^2\{\cos(2\theta - 2\theta_r) + Rcos(2\theta)\}}{1 + R^2 + 2Rcos(\theta_r)}\right]cos(\theta)d\theta,$$

$$F_d = \frac{24\pi\mu{R_d}^2U_d}{h}.$$

References

(1) Skowronek, V.; Rambach, R. W.; Schmid, L.; Haase, K.; Franke, T. *Anal Chem* **2013**, *85*, 9955-9959.
(2) Schmid, L.; Weitz, D. A.; Franke, T. *Lab Chip* **2014**, *14*, 3710-3718.
(3) Ma, Z.; Collins, D. J.; Ai, Y. *Anal Chem* **2016**, *88*, 5316-5323.
(4) Park, J.; Jung, J. H.; Destgeer, G.; Ahmed, H.; Park, K.; Sung, H. J. *Lab Chip* **2017**, *17*, 1031-1040.

Movie captions:

Supplementary Movie 1: Acoustic droplet bi-splitting
Supplementary Movie 2: Acoustic droplet steering
Supplementary Movie 3: Acoustic droplet tri-splitting